EPSC Abstracts
Vol. 8, EPSC2013-987, 2013
European Planetary Science Congress 2013

Fault scaling on Mars: Slip distribution and displacement-length relationship derived from HRSC data

E. Hauber, M. Voelker, K. Gwinner, M. Knapmeyer, M. Grott and K.-D. Matz
DLR-Institut für Planetenforschung, Berlin, Germany (Ernst.Hauber@dlr.de / Fax: +49-30-67055-402)

Abstract

We determined the slip distribution along normal faults on Mars, using Digital Elevation Models (DEM) and corresponding orthoimages derived from High Resolution Stereo Camera (HRSC) data. Typically, the slip distribution along faults displays a peak or maximum displacement (D_{max}) approximately midway along the fault trace length (L), whereas displacement minima may indicate segment linkage via relay ramps or local phenomena such as cross-cutting with other fault sets. The fault scaling displays a large scatter and follows a relationship of $D_{max} \approx 0.01 \cdot L$, consistent with results for terrestrial faults. Our measurements show a slightly higher D_{max}/L ratio than previous studies of planetary faults. We ascribe this to our use of high-resolution topographic data, because the location of D_{max} may be underestimated when using lower-resolution data.

1. Introduction

Geometric fault properties can provide insights into the mechanical and temporal evolution of fault systems [1,2] and the past and future potential for seismic energy release [3]. In planetary science, where a lack of seismometers is unfortunately the rule rather than the exception, the analysis of faults with remote sensing data typically provides the only direct observational evidence to constrain the tectonic history of a planet [4]. Since the seismic moment released during the growth of a fault is strongly connected to the fault geometry, the study of fault populations can also help to estimate the current seismicity level [5,6]. Until today, however, only few data on the relationships between fault displacement and length have been collected for extraterrestrial bodies [8], partly due to the limited number of reliable topographic datasets. Here we use DEM and orthoimages from HRSC [9] to obtain information on the displacement distribution along fault traces. This also enabled determining the maximum displacement. We compare our results to previous measurements of faults on Mars, Earth, and other planets. Based on these analyses, we discuss the implications of fault segmentation and linkage for further interpretation.

2. Data and methods

All measurements on fault geometry were made in HRSC DEM and orthoimages. Individual DEM have typical grid sizes of 50 to 100 m, corresponding orthoimages have resolutions of 12.5 to 25 m px^{-1}. For detailed structural interpretation of key locations (e.g., relay ramps), MOC (~3-5 m px^{-1}) and CTX (~5-6 m px^{-1}) images have been inspected where available. Fault length was digitized along the fault line, and multiple topographic cross-sections across the fault were drawn with a spacing of ~1 km. Fault throw (as a proxy for true displacement) was visually determined in the digitized cross-sections.

3. Results

The locations of study areas were determined by the availability of HRSC DEM with high accuracy. We focused on the following areas in and around Tharsis: Alba Mons (E flank), Tempe Terra, Ophir Planum, and Claritas and Tantalus Fossae. The most challenging aspect was the identification of individual faults or fault segments with little evidence for degradation and cross-cutting relationships with other faults. Although fault growth by segment linkage clearly appears to be an important process in the evolution of Martian fault populations (Fig. 1), faults were only considered to be linked when clear morphologic evidence such as breached relay ramps were observed (Fig. 2). The length range of faults for which the displacement could be determined spans about 1.5 orders of magnitude (Fig. 3a). Up to the time of writing (May, 2013), no faults shorter than a few kilometers could be reliably measured. The D/L ratio is in the order of 10^{-2} (Fig. 3a), consistent with values determined for terrestrial faults (Fig. 3b) [9].

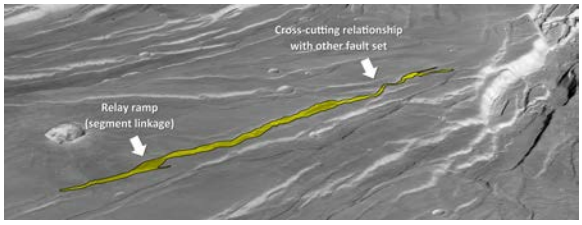

Figure 1: Perspective 3D-view of normal faults in Tempe Terra, Mars (center at 39.13°N/285.89°E, view is toward N, sun from right). Note many relay ramps linking fault segments. The fault shown in Fig. 2 is highlighted in yellow (image width ~ 100 km).

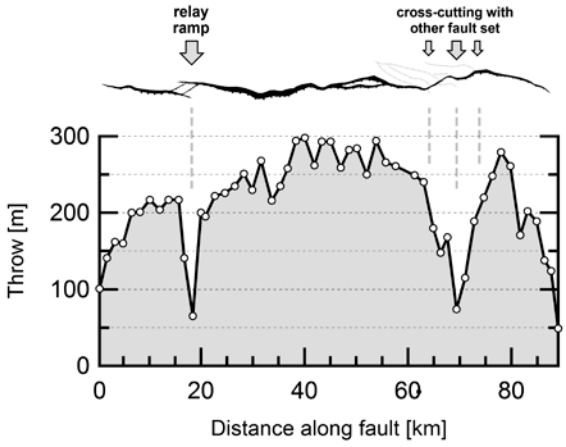

Figure 1: Normal fault *(top)* and associated slip distribution *(bottom)*. Note that distinct minima are associated with a relay ramp (left) and a location where the fault is cross-cut by another fault set.

4. Summary and Conclusions

Our preliminary results show that the displacement profiles of normal faults on Mars bears information on the evolution of faults by segment linkage (see also [11]). The D_{max}/L ratio is roughly centered at a value of 10^{-2}, which is also observed for terrestrial faults, but slightly higher than some previous estimates for planetary D_{max}/L ratios. This may result from improved D_{max} determination in highly resolved DEM. Our data display a large scatter, and we found it difficult to measure faults shorter than ~5 km. This may attributed to the fact that Martian faults are rarely observed in bedrock and, therefore, small faults would appear "blurred" in regolith. Extension of our approach to bedrock (e.g., layered deposits in Valles Marineris) might mitigate this problem and extend the length range of analyzed faults.

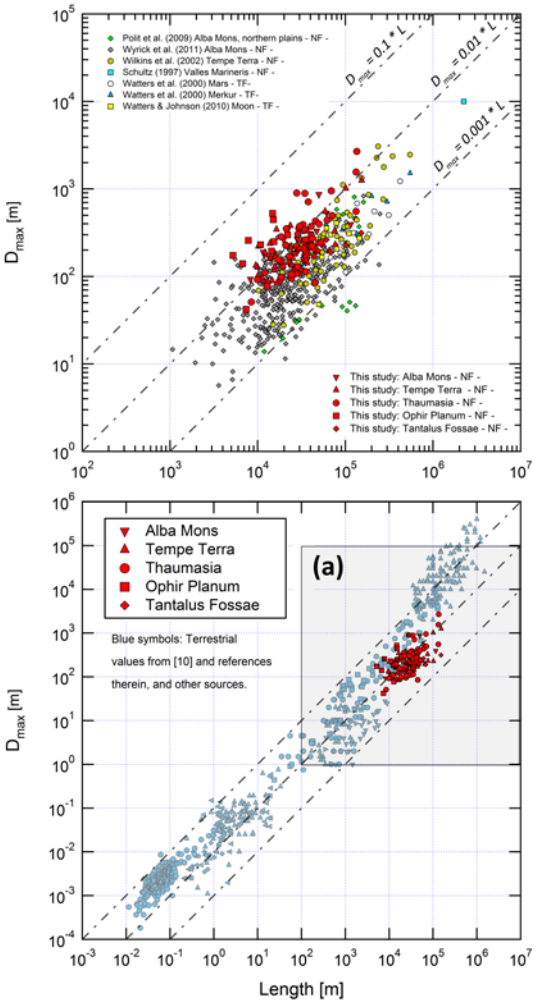

Figure 3: Maximum displacement vs. fault length.

Acknowledgements

Displacement data for Earth and Mars have been kindly provided by R. Schlische and D. Wyrick. This study was supported by the Helmholtz Alliance "Planetary Evolution and Life".

References

[1] Cartwright, J. A., et al., *J. Struct. Geol.* **17**, 1319-1326, 1995. [2] Cowie, P.A. and Scholz, C.H., *J. Struct. Geol.* **14**, 1133-1148, 1992. [3] Wells, D.L. and Coppersmith, K.J., *Bull. Seismol. Soc. Amer.* **84**, 974-1002, 1994. [4] Schultz, R.A., et al., *J. Struct. Geol.* **32**, 855-875, 2010. [5] Golombek, M.P., et al., *Science* **258**, 979-981, 1992. [6] Knapmeyer, M., et al., *J. Geophys. Res.* **111**, E11006, 2006. [7] Schultz, R.A., et al., *J. Struct. Geol.* **28**, 2182-2193, 2006. [8] Gwinner, K. et al., *Earth Planet. Sci. Lett.* **294**, 506-519, 2010. [9] Scholz, C.H., *Int. J. Rock Mech. & Min. Sci.* **34**(3-4), Paper No. 273, 1997. [10] Schlische, R.W., et al., *Geology* **24**, 683-686, 1996. [11] Wyrick, D.Y., et al., Icarus 212, 559-567, 2011.